Sensors & Actuators: B. Chemical 325 (2020) 128789

Contents lists available at ScienceDirect

Sensors and Actuators: B. Chemical

journal homepage: www.elsevier.com/locate/snb

Peptide decorated gold nanoparticle/carbon nanotube electrochemical sensor for ultrasensitive detection of matrix metalloproteinase-7

Quentin Palomar [a], XingXing Xu [a], Robert Selegård [b], Daniel Aili [b,*], Zhen Zhang [a,*]

[a] Division of Solid-State Electronics, Department of Electrical Engineering, The Ångström Laboratory, Uppsala University, P.O. Box 534, SE-751 21, Uppsala, Sweden
[b] Laboratory of Molecular Materials, Division of Biophysics and Bioengineering, Department of Physics, Chemistry and Biology (IFM), Linköping University, SE-581 83, Sweden

ARTICLE INFO

Keywords:
Biosensor
Carbon nanotubes
Gold nanoparticles
Peptide
MMP-7
Gold electrode
Differential pulse voltammetry

ABSTRACT

Matrix Metalloproteinase-7 (MMP-7) is a proteolytic enzyme overexpressed in different pathological conditions, including cancer, infection, and cardiovascular diseases, and is a relevant diagnostic biomarker and potential drug target. Here we demonstrate rapid and selective detection of MMP-7 with a limit-of-detection of 6 pg/mL and a dynamic range from 1×10^{-2} to 1×10^{3} ng/mL using a peptide decorated gold nanoparticle/carbon nanotube electrochemical sensor. The sensor could be operated in diluted human serum and synthetic urine, with high specificity towards MMP-7. Moreover, the integration of nanomaterials in the sensing electrode significantly increased the signal-to-background ratio and strongly improved the stability of the sensor when compared to a conventional gold electrode. The simple and cost-effective fabrication and the ease of use make this sensor a very promising protease detection device for diagnostics and drug development.

1. Introduction

Sensitive detection of biological macromolecules is vital for biomedical research, drug development, diagnostics and numerous other bioanalytical applications. Development of biosensors capable of rapid and selective detection of specific biomolecular targets of interest, such as DNA, antibodies and other proteins have thus intensified during the last decade [1,2]. Because of their central role in both healthy tissues and disease, detection of proteases and especially matrix metalloproteinases (MMPs) has been one of the focus directions in biosensor development. This group of enzymes are involved in a large number of different pathological conditions, such as several forms of cancer, infection, and cardiovascular diseases [3,4]. During the manifestation of such pathologies, MMPs tend to be upregulated and are therefore relevant drug targets and biomarkers. Consequently, there is need for reliable and sensitive tools for monitoring concentration and activity of MMPs. Different methods have been developed for detection of MMPs, such as the commonly used enzyme-linked immunosorbent assay (ELISA) [5], electrophoretic techniques [6] and optical methods such as enhanced chemiluminescence (ECL) [7]. However, these techniques have limitations with respect to availability, operating cost, response time, selectivity and sensitivity. In addition, affinity-based techniques, such as ELISA, only measure MMP concentration rather than enzyme activity [8].

Electrochemical transduction strategies are widely used in biosensors [9] and offers many advantages, such as rapid analysis, instrument miniaturization, and low running cost, compared to most conventional laboratory techniques. Electrochemical biosensors are also very versatile, since the surface of the electrode can be modified with different kinds of bioreceptors that are specific to the analytes of interests. Regarding the detection of MMPs, different groups have recently developed electrochemical biosensors based on MMP-mediated peptide cleavage [10–12]. The change in the electrochemical current intensity triggered by the hydrolysis of a peptide substrate by the MMP enables rapid label-free detection. In addition to the low cost of peptides compared to other types of bioreceptors such as antibodies, they can be tailored for specific MMPs and enable site directed immobilization on a sensor substrate. Peptides can also be produced in large quantities using solid phase peptide synthesis, and have long shelf-life, which not only reduces the costs of a sensor but also facilitates sensor handling and storage.

Enzymatic cleavage of peptides immobilized on an electrode surface results in release of peptides fragments from the surface. This will facilitate the electron transfer between the electrode and the

* Corresponding authors.
E-mail addresses: daniel.aili@liu.se (D. Aili), zhen.zhang@angstrom.uu.se (Z. Zhang).

https://doi.org/10.1016/j.snb.2020.128789
Received 2 June 2020; Received in revised form 18 August 2020; Accepted 19 August 2020
Available online 21 August 2020

electroactive species in the liquid sample thus increasing the intensity of the electrochemical current. However, the small size of the released peptide fragments results in a very small change in term of current intensity. The use of an electrochemical signal amplifier is therefore essential. Several groups have used enzymatic or metallic catalytic reactions to increase the intensity of the signal, such as Zheng et al. [13]. Another approach consists of using nanomaterials as signal amplifier [14]. Nanomaterials can significantly increase the specific surface area due to their large surface-to-volume ratio, resulting in a large and highly accessible interface between the electrolyte and the electrode. In addition, they have very interesting intrinsic properties such as electrical conductivity and chemical reactivity that can be exploited in the design of biosensors. In the presented work, we have explored a nanocomposite of carbon nanotubes (CNTs) and electrogenerated gold nanoparticles (GNPs) as the signal amplifier for sensitive detection of protease activity using a designed peptide substrate (JR2EC) [15]. CNTs, because of their intrinsic properties and more particularly their very good electrical conductivity and large surface area, represent a material of choice for the design of electrodes [16]. The advantage of carbon compounds also lies in the fact that they offer a wide selection of chemical modification and can easily be combined with other nanocompounds such as GNPs. Recently, several groups have also taken advantage of the properties of carbon materials as base frame for producing nanostructured electrodes [17,18]. In this work, we show that the combination of these two materials resulted in a nanocomposite electrode with a substantially enhanced sensing signal compared to a conventional gold sensing electrode. This enhancement increased the signal-to-background ratio (S/B) and lowered the limit-of-detection (LOD) for MMP-7 detection. We also found that the nanocomposite electrode had excellent stability without any of the electrochemical current drift typically seen in a conventional electrode [19,20]. Moreover, this strategy offers a very rapid acquisition time (30 min), which makes this sensor an interesting alternative to more time-consuming devices presented in the literature or to the classic ELISA tests ($\geq$ 90 min). Finally, it requires a very small amount of samples from the patient and does not require strong logistics or expensive laboratory devices. Ease of use and ease of engineering are indeed often the key parameters left out when designing biosensors, despite that both simple use and rapid detection are essential for effective diagnosis in the field [21]. In summary, we present here a versatile system allowing rapid, simple and sensitive detection of biomolecules in complex media while addressing the key problems related to the electrochemical sensor, namely system stability and selectivity. The operating principle of the sensor is schematically illustrated in Fig. 1.

2. Experimental section

The electrodes were first modified by a thin layer of CNT before electrogeneration of GNP by chronoamperometry. The peptide was immobilized on the as-modified nanocomposite electrodes using gold-thiol chemistry. After careful rinsing of the electrodes, the electrodes were incubated in a solution containing 0.01 ng/mL–1 µg/mL MMP-7 spiked in either phosphate buffered saline (PBS), human serum or synthetic urine. The electrodes were immersed for 30 min in the corresponding solution at room temperature to perform the enzymatic reaction. Detection was performed afterward in 3 mM $K_4[Fe(CN)_6]^{4-}$/$K_3[Fe(CN)_6]^{3-}$ (1:1) in 1xPBS solution pH = 7.4. A more detailed experimental procedure and materials can be found in NOTE S1 in the supplementary information (SI).

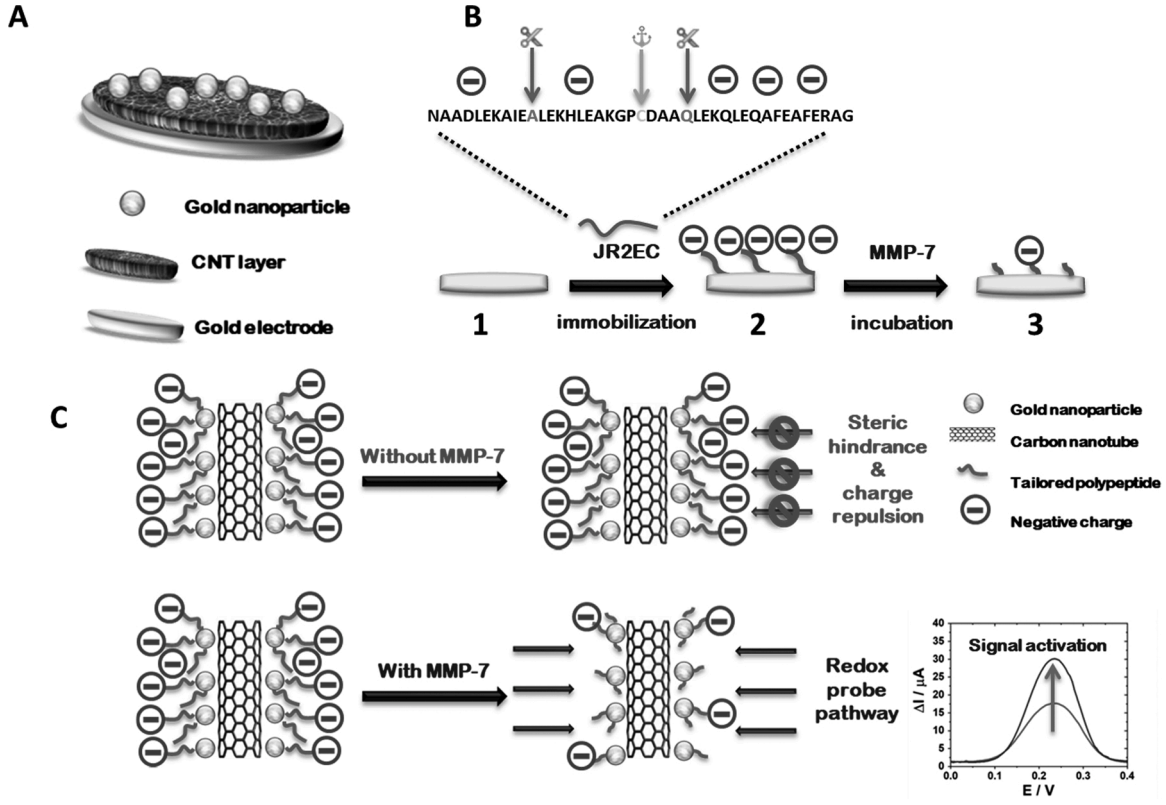

Fig. 1. (A) Schematic representation of the structure of the sensor. (B) Schematic representation of the different steps involved in the construction of the biosensor with the gold electrode before immobilization of the polypeptide (1), after immobilization of the peptide (2) and after reaction with MMP-7 (3). (C) Schematic illustration of the operating principle of the sensor: the immobilized polypeptide blocks the redox probe and inhibits the electrochemical signal, and its cleavage in the presence of MMP-7 results in signal activation. The intensity of the corresponding electrochemical signal is also reported on the presence (blue) or absence (red) of enzyme. (For interpretation of the references to colour in this figure legend, the reader is referred to the web version of this article).

3. Results and discussion

3.1. Sensing electrode evaluation

The electrochemical response of the nanocomposite sensor was investigated by cyclic voltammetry (CV) and differential pulse voltammetry (DPV) and compared to a conventional planar gold electrode, before and after immobilization of JR2EC and subsequent treatment with 1 μg/mL of MMP-7 (Fig. 2A and B).

A large difference in term of current intensity between the conventional planar gold electrode and the nanocomposite electrode modified by the CNT/GNP nanocomposite was seen. The voltammograms showed well-defined redox peaks for both systems with an intensity of 0.0057 mA for the unmodified gold electrode and 0.345 mA for the nanocomposite electrode. The electrochemical current recorded was hence increased by a factor > 60 for the nanocomposite electrode compared to the conventional planar gold electrode. This difference can be explained by the large surface-to-volume ratio of the CNTs and GNPs in combination with the highly porous structure of the network of interconnected CNTs (see Fig. S1), which results in a larger interface for

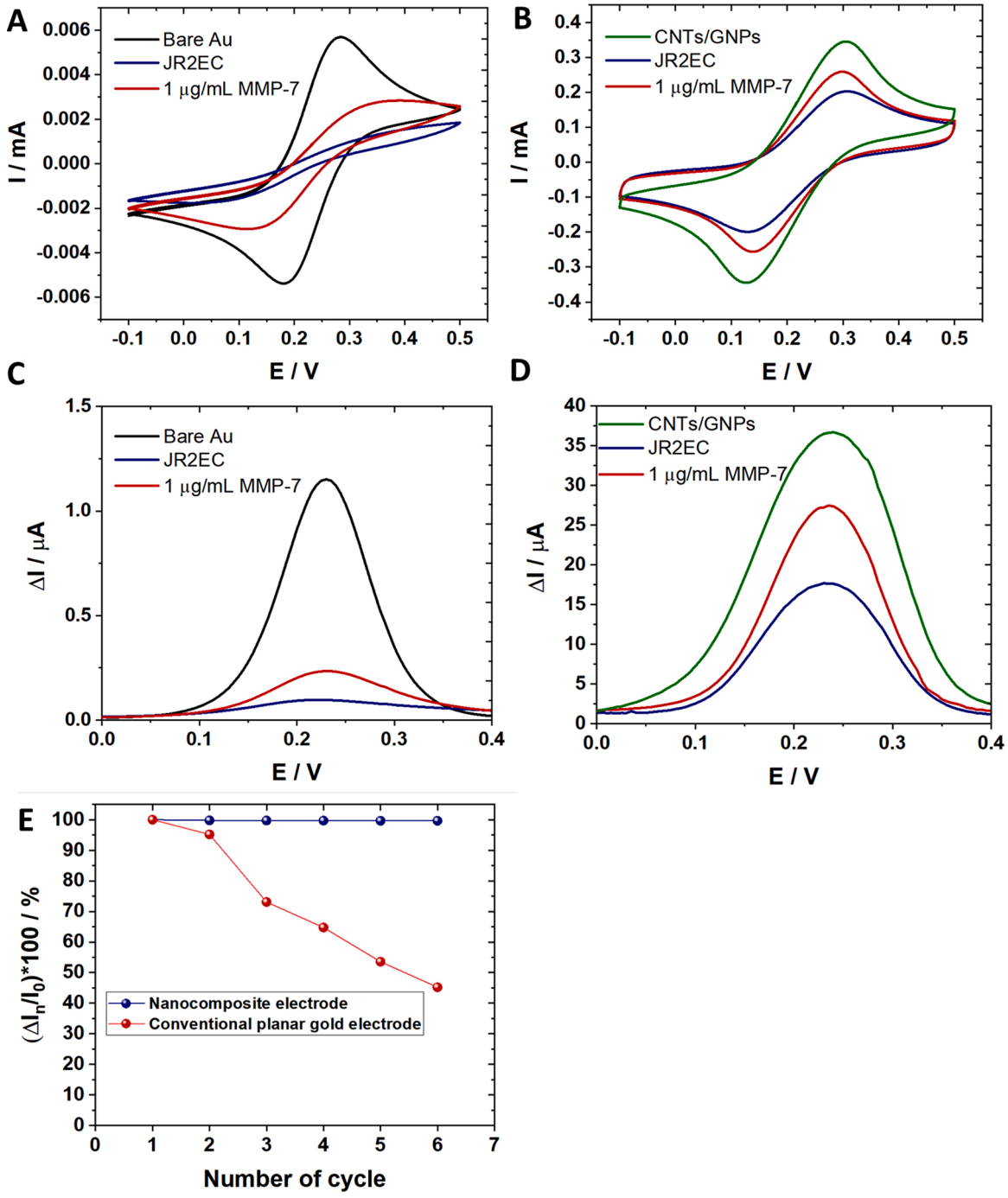

Fig. 2. (A) Cyclic voltammograms and performed on a conventional planar electrode and on a nanocomposite electrode (B) in 3 mM $K_4[Fe(CN)_6]^{4-}/K_3[Fe(CN)_6]^{3-}$ (1:1) in 1xPBS solution pH = 7.4. Scan rate: 100 mV s^{-1}. (C) Differential pulse voltammograms performed on a conventional planar electrode and on a nanocomposite electrode (D). For DPV measurements, a pulse height of 2.5 mV and a width of 100 ms were used along a step height of 5 mV and a step time of 500 ms. (E) Normalized DPV current to initial DPV current ratio under repeated measurements in 30 min intervals in 0.1 M PBS solution containing 3 mM $[Fe(CN)_6]^{3-/4-}$, for a planar gold electrode and a nanocomposite electrode after JR2EC immobilization.

the electron transfer compared to the conventional planar surface. At room temperature, an area of 0.0064 cm^2 was calculated for the conventional planar gold electrode and 1.348 cm^2 for the nanocomposite electrode, or an area increased by 210 times after the integration of nanomaterials. The detailed calculation can be found in SI (NOTE S2).

After immobilization of JR2EC, also shown in Fig. 2A and B, sharp decreases in the current intensities were observed, from 0.345 mA to 0.202 mA and from 0.0057 mA to 0.0015 mA for the nanostructured and conventional planar gold electrode, respectively. A surface JR2EC coverage of 1.49×10^{-10} mol/cm^2 for the conventional planar gold electrode and 3.41×10^{-10} mol/cm^2 for the nanocomposite electrode were determined using reductive desorption (Fig. S2). The current drop observed is due to the electron transfer hindering effect of the peptide. The presence of the peptide results in steric hindrance that restricts the diffusion of the redox probe through the porous network, decreasing the available surface area for the electronic exchange between the electrode and the probe. Moreover, the net charge of polypeptide results in electrostatic repulsion of the $[Fe(CN)_6]^{3-/4-}$. The blocking of the planar electrode was more efficient, as shown by the relative variation of the current intensity, since the peptide covers the entire surface. On the conventional electrode, the peptide efficiently blocks the entire surface of the electrode. In contrast, on the nanocomposite, the peptide is primarily bound to the GNPs and electron transfer can still occur via the structure of CNTs electrode. This effect also results in a larger relative increase in the current for the planar electrodes when exposed to 1 μg/mL MMP-7, from 0.0015 to 0.0028 mA (87 % increase), compared to the increase from 0.202 to 0.259 mA (28 % increase) on the nanocomposite surface. Despite the smaller relative current increase, the much larger absolute current increase induced by MMP-7 (sensing signal) in the nanocomposite electrode can greatly benefit the S/B of the sensor since the background fluctuation of electrochemical measurements is around 0.05 μA for both electrodes.

The same general behaviors were observed by DPV. Compared to conventional cyclic voltammetry, DPV reduces the impact of capacitive current and allows for detection of lower concentrations of the target analyte [22]. By DPV, the current intensity recorded is directly related to the faradaic contribution and reflects more accurately the phenomena occurring between the redox probe and the electrode, i.e. the electron transfer. This is hence a more precise technique when it comes to detection of low concentrations and small changes at the interface.

Regarding the intensity of the oxidation peak prior to immobilization, Fig. 2C shows a peak at 1.15 μA for the planar gold electrode and the Fig. 2D a peak at 36.7 μA for the nanocomposite electrode. Once the polypeptide was immobilized, a decrease in the current intensity was observed for both systems, 17.6 and 0.096 μA for the nanocomposite and planar electrodes, respectively. This confirmed the observations from CV. It may be noted that the difference between the current obtained before and after peptide immobilization was striking for both sensors and clearly shows the influence of JR2EC on slowing the electron transfer. The relative current intensity was reduced by 50 % on the nanocomposite electrode after the polypeptide immobilization, and by 90 % on the planar electrode.

When the electrodes were exposed to MMP-7 (1 μg/mL), an increase of the differential current from 17.6 μA to 27.4 μA and from 0.096 μA to 0.23 μA was observed for the nanocomposite electrode and the planar electrode, respectively. The sensing signal (the absolute differential current increase $\Delta I_S = \Delta I_n - \Delta I_0$, where ΔI_0 is the reference differential current intensity obtained after the polypeptide immobilization and ΔI_n is the differential current intensity obtained after MMP-7 reaction) generated in the nanocomposite electrodes significantly larger. This resulted in a significantly improved S/B in the nanocomposite electrodes (196) when compared with the planar electrodes (2.68). The improved S/B can facilitate discrimination of the redox signal from the background fluctuations and increase the dynamic range of the sensor, which will be demonstrated later.

Since sensor drift is a common problem in electrochemical sensors that can result in false positives [19], the stability of the two types of electrodes was tested by incubating the electrodes in a solution of 3 mM $[Fe(CN)_6]^{3-/4-}$ in 0.1 M PBS solution for 30 min after peptide immobilization. Subsequently, successive electrochemical measurements were performed at 30 min intervals using DPV in presence of the redox probe. The electrodes were kept immersed in the measurement solution between cycles. The differential current values were normalized to their initial value (the first cycle) for both electrode systems to compare their stability, since the nanocomposite electrode having much higher current intensity than the planar gold electrode. As shown in Fig. 2E, significant difference in stability was seen between the two electrode systems. For the conventional planar gold electrode, a rapid decrease of the current ratio was observed after successive measurements. A 50 % total decrease from the initial current was recorded after 5 cycles in a solution of 3 mM $[Fe(CN)_6]^{3-/4-}$. In contrast, the nanocomposite electrode remained very stable, showing a modest drop of only 0.5 % from the initial current after 6 cycles. Two reasons can potentially lead to the better stability of the nanocomposite electrode. First, as shown by different studies, several species can adsorb on the surface of a gold electrode when immersed in a $[Fe(CN)_6]^{3-/4-}$ solution. Dijksma et al. have shown that the presence of CN- ions, released by the redox couple, can lead to the formation of $[Au(CN)]^{2-}$ complex and hindered the electronic transfer [23,24]. Other studies have reported possible passivation of the gold surface by the adsorption of HPO_4^{2-} [25]. This anion can induce a repulsion of the redox probe, due to its negative charge, and can explain the current decrease. Second, this effect will be more pronounced for the conventional planar electrode than for the nanocomposite electrode. For the nanocomposite electrode, the drift is still present but only up to 0.5 % of the initial current, since the current is mainly contributed by the charge transfer on the CNTs and the possible drift on the GNP surface have much smaller impact on the total current.

Overall, the nanocomposite electrodes can perform better than the conventional planar gold electrode in MMP-7 sensing with respect to both S/B, stability and reliability. In addition, since DPV more accurately detects the electron transfer and hence is a more precise technique for detection of low concentrations and small changes at the interface, for the rest of the study, only the nanocomposite electrode and DPV were used.

3.2. Detection of MMP-7 in PBS

In order to investigate the performance of the proposed biosensor, the JR2EC functionalized nanocomposite electrodes were exposed to different concentrations of MMP-7 ranging from 0.01 ng/mL to 1 μg/mL. For each concentration, the incubation time was kept constant (30 min) and the electrodes were rinsed thoroughly using PBS solution between each measurement. Different incubation times have been tested and 30 min was found to be the optimal time to allow a complete reaction of the enzyme. The DPV voltammograms for these different concentrations and the corresponding calibration plot are presented in Fig. 3A and B respectively. The intensity of the differential current increased as a function of the enzyme concentration increase (Fig. 3A). A higher concentration of enzyme results in a more extensive degradation of the peptide in the same time interval (30 min) and therefore higher electron transfer. Multiple runs were carried out for each concentration on 3 different electrodes to ensure the reproducibility of the results.

Fig. 3B shows the sensor response as a function of the logarithm of MMP-7 concentration. In our system, the increase in differential current intensity caused by the increased enzyme concentration did not follow the classical model for enzymatic reaction described by Langmuir but rather the Temkin isotherm [26]. The Temkin model takes into account the inhomogeneity of the different adsorption sites and was initially used to describe a heterogeneous protein adsorption. With this model, a semi-logarithmic dependence between the sensing signal ΔI_s and MMP-7 concentration was observed in the concentration range from 1×10^{-2} to 1×10^{3} ng/mL ($r^2 = 0.973$). The LOD, defined by 3 x standard deviation

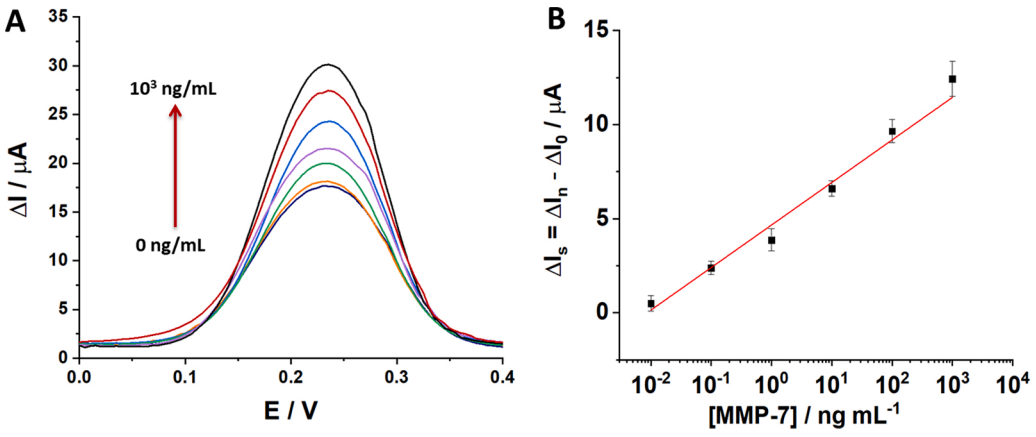

Fig. 3. A) DPV curves after incubating the nanocomposite electrodes with various concentrations of MMP-7 in PBS solution. From bottom to top: 0, 0.01, 0.1, 1, 10, 100 and 1×10^3 ng/mL. B) Calibration plot for the biosensor corresponding to the changes in current intensity after incubation with MMP-7 at different concentrations in buffer solution. Experimental data obtained on 3 different electrodes (dots) and linear regression (line) are presented. Linear regression: $y = 1.0445\ \ln(x) + 4.70$; $R^2 = 0.9843$. For DPV measurements, a pulse height of 2.5 mV and a width of 100 ms were used along a step height of 5 mV and a step time of 500 ms.

of the blank, was 6 pg/mL. As shown in Table 1, several papers report a lower LOD for MMP-7. Yun Zheng et al. [13] demonstrated a palladium nanoparticle (PdNP) based sensor with an LOD of 0.0031 pg/mL. The PdNPs were used as catalytic entities to perform a two-step detection of the target analyte. Albeit very sensitive, this strategy required the addition of different reagents and a complicated surface chemistry involved in the detection but also the operation of the sensor. In comparison, the works described in this paper offered a higher LOD but did not require any labeling or secondary reaction to perform the detection. This facilitates the operation of the biosensor and reduces the acquisition time, which are important parameters for a point of care application. Other works such as Ding Wang et al. [27] and Bei-Bei Kou et al. [28] have taken advantage of similar amplification principle. This kind of system, however, may be difficult to implement since they require multiple steps and the addition of different chemicals in order to perform the detection. This type of device is therefore not perfectly suited for point of care and portable device type applications.

The nanocomposite sensor presented in this work offers a very wide dynamic range, covering 6 orders of magnitude from 1×10^{-2} to 1×10^3 ng/mL. The concentration of MMP-7 in a healthy tissue is typically in the interval 0.1–3.5 ng/mL [33,34]. In pathological conditions, the concentration can increase up to 10−15 ng/mL in urine sample [35] and serum sample [36] for patient with bladder cancer. The dynamic range of our sensor is thus sufficient to cover the relevant concentrations for medical diagnostics. Moreover, our system is very user-friendly with a one-step detection process and a short acquisition time compared to most of the papers found in the literature, which is mandatory for a point of care device. Indeed, many works proposed detection systems with assay times longer than the commercially available ELISA kits (≥90 min), reducing the advantage of using a biosensor. The stability and ease of use are determining factors in the design of a biosensor in order to meet the criteria of speed and portability of field tests. In addition, the electrochemical detection and the materials used here are very cheap and therefore allow for a low cost fabrication.

The specificity of the system was investigated by exposing the biosensor to different proteins. Urease, Bovine Serum Albumine (BSA) and deactivated MMP-7 were tested, as well as a mixed solution comprising urease, BSA and active MMP-7. The different proteins were all tested at a concentration of 1 μg/mL in PBS solution. Deactivation of MMP-7 was done by exposing the enzyme to an EDTA solution (20 mM), which removes the catalytic Zn^{2+} from the active site. Fig. 4 shows the relative response generated by different samples, $R = [(\Delta I_n - \Delta I_0)/\Delta I_0] * 100$, where ΔI_0 is the reference differential current intensity obtained after the polypeptide immobilization and ΔI_n is the current obtained after incubation with the different protein samples.

As shown in Fig. 4A, the responses observed after incubation with BSA (5 %) and urease (2 %), were significantly lower as compared to the response from samples spiked with MMP-7 (71 %). The deactivation of MMP-7 using EDTA efficiently inhibited the ability of the enzyme to cleave the polypeptide, resulting in a significant drop in the response (5 %). It may also be noted that the relative response obtained for the mix solution containing both urease (1 μg/mL), BSA (1 μg/mL) as well as MMP-7 (1 μg/mL) was similar (72 %) to the one obtained for MMP-7 alone, indicating limited effects caused by any unspecific adsorption of these proteins on the sensor surface.

Moreover, no significant interference (5 %) on the redox peak current was observed after exposing the sensor to more complex media, such as human serum and synthetic urine. (Fig. 4B). In contrast, addition of MMP-7 (1 μg/mL) to the serum and the synthetic urine resulted in a significant increase in the relative response of 49 % and 42 % in human

Table 1
Comparison of the performances of different nanostructured electrochemical MMP-7 biosensors.

	System used	Detection technique	Number of steps	Assay time / min	LOD/ ng/ mL	Linearity/ ng/ mL	Measurement in complex media
This work	GE/MWCNTs/GNPs	DPV	1	30	6×10^{-3}	0.01−1000	Yes
Hongfang Gao et al. [29]	Peptide labelled with two metal complexes as luminophores	ECL	1	60	1×10^{-2}	0.05−1	Yes
Zheng Wei et al. [30]	Pd-functionalised carbon nanocomposite	Square Wave Voltammetry (SWV)	2	110	1.7×10^{-5}	0.0001−100	No
Ding Wang et al. [27]	Magnetic peptide – DNA probe	SWV	3	110	2×10^{-5}	0.0001−50	No
Zhen Lei et al. [31]	Au/Ag-SiO_2	Field Effect Transistor	1	≥ 60	2.2×10^{-4}	0.01−100	Yes
Bei-Bei Kou et al. [28]	DNA enzyme-decorated DNA nanoladders	DPV	3	105	5×10^{-5}	0.0002-20	No
Yun Zheng et al. [13]	Au-reduced graphene oxyde + Pd nanoparticles	SWV	3	≥ 100	3.1×10^{-6}	0.00001−10	Yes
Wei Zhuang et al. [32]	Copper nanocluster-labeled hybridization chain	Potentiometric immunoassay	3	≥ 90	5.3×10^{-3}	0.01−100	Yes

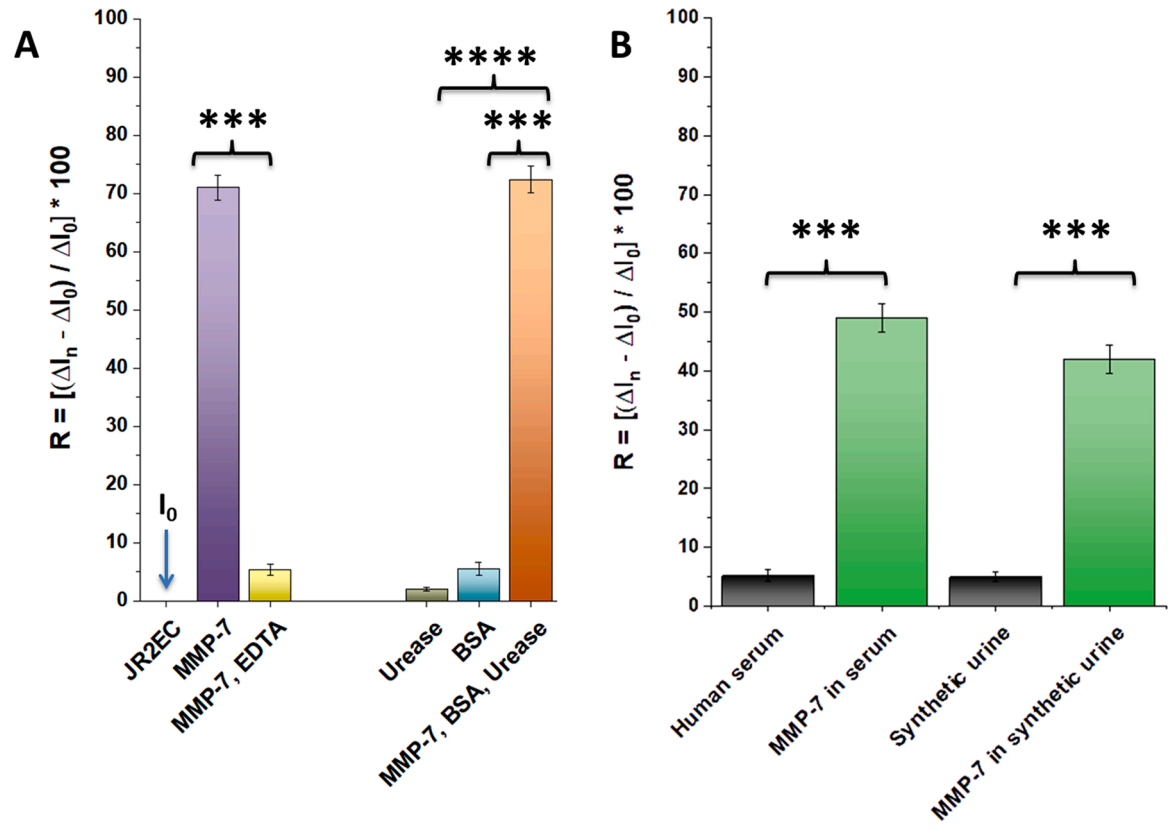

Fig. 4. The relative response in the nanocomposite electrodes generated by different biomolecules (A) 1 µg/mL mg/mL urease, 1 µg/mL mg/mL bovine serum albumin (BSA), 1 µg/mL MMP-7 deactivated with EDTA (MMP-7-EDTA), 1 µg/mL active MMP-7 (MMP-7) and a mix solution comprising 1 µg/mL urease, 1 µg/mL BSA and 1 µg/mL MMP-7 in PBS solution. (B) The sensor response in complex media (human serum and synthetic urine) with 1 µg/mL of MMP-7 and without MMP-7 is also presented. Respective *t*-test results are shown (3 stars: $P \leq 0.001$; 4 stars $P \leq 0.0001$).

serum and synthetic urine, respectively. The sensor can thus be efficiently operated and detect MMP-7 activity in complex media of relevance for diagnostics.

The lifetime of the sensor was also investigated. After being stored for 5 weeks in PBS, the sensor exhibits a decrease in the response signal to MMP-7 of only 10 %. The system therefore allows medium-term storage up to one month (Fig. S3).

3.3. MMP-7 assay in human serum and synthetic urine

To provide a model close to real sample applications conditions, the sensing platform was applied to the detection of MMP-7 in different physiological fluids, including human serum and synthetic urine. The experimental conditions were optimized to promote the electrochemical signal in these different environments. The nanocomposite electrodes were conditioned for 20 min in the corresponding medium and the DPV parameters were optimized to increase the reading of the signal. The human serum, a complex medium with a high viscosity, was also diluted 1:100 in PBS to facilitate the experiment.

Both media were spiked with MMP-7 at concentrations ranging from 0 to 1×10^3 ng/mL. The study was performed on 5 different electrodes.

As shown in Fig. S4A, as the concentration of MMP-7 increased in human serum, an increase in the peak current was observed, similar to the results observed in PBS solution. An increase of the differential current peak of 16 µA was seen when the MMP-7 concentration was raised from 0 to 1×10^3 ng/mL. In addition, the recorded data again agree with the Temkin model, exhibiting a correlation factor of 0.983. It is important to note that the concentration range observed here is also sufficient to cover the diagnostic needs for a MMP-7 sensor since the concentration varying from 0.1 ng/mL in a healthy patient to 15 ng/mL in serum sample from a patient suffering from bladder cancer [36].

MMP-7 detection was also performed in synthetic urine without dilution. The redox peak current increased with increasing MMP-7 concentration (Fig. S4B). The calibration curve of the response of the biosensor for MMP-7 is shown in Fig. 5B. The total increase in the differential current peak when the MMP-7 concentration was increased from 0 to 1×10^3 ng/mL is very similar to the increase obtained from the serum sample (14.8 µA). This highlights the reproducibility of the biosensor presented in this paper as well as its ability to operate in various complex media. In addition, the dynamic range tested covers the detection range required for real urine tests [35]. All of these different results are promising for the use of this sensor for clinical samples and for the development of point of care detection device based on this work.

4. Conclusion

A label free biosensor for the detection of MMP-7 was prepared by modifying a gold electrode with a nanocomposite based on CNTs and GNPs. This nanostructured surface acted as a signal amplifier that resulted in a significant improvement in both S/B and stability, compared to a conventional planar gold electrode. The nanocomposite electrode was further modified with a peptide containing two cleavage sites for MMP-7. The hydrolysis of the immobilized peptide was monitored using a sensitive electrochemical technique (DPV). A limit of detection of 6 pg/mL was obtained and the sensor could operate over a wide concentration range (1×10^{-2}–1×10^3 ng/mL). In addition, this biosensor exhibited a very good selectivity towards MMP-7 and a very good stability. The detection of MMP-7 was also carried out in the presence of human serum and synthetic urine, demonstrating the potential of the biosensor for clinical applications. Due to its ease of use, its low production cost and its excellent performances, this system is very promising for the development of a point of care device and for early

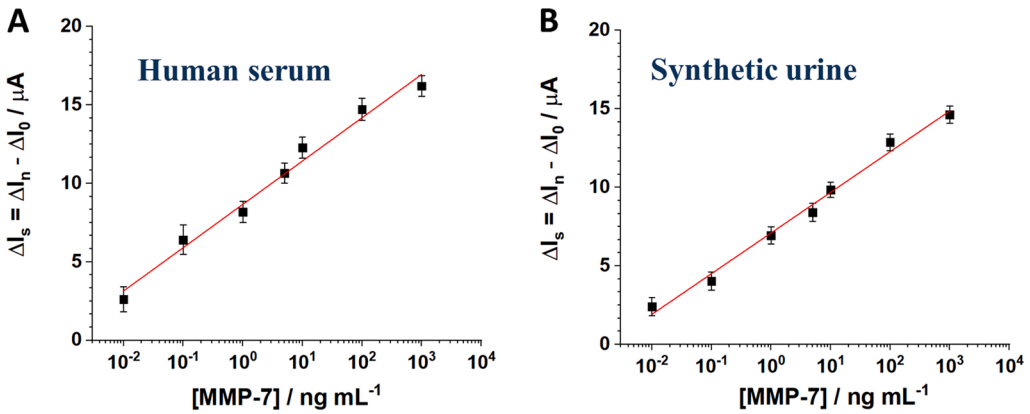

Fig. 5. A) Calibration plot for the biosensor corresponding to the changes in current intensity after incubation with MMP-7 at different concentrations in diluted human serum. Linear regression: $y = 1.2034\ln(x) + 8.68$; $R^2 = 0{,}983$. B) Calibration plot for the biosensor corresponding to the changes in current intensity after incubation with MMP-7 at different concentrations in synthetic urine. Linear regression: $y = 1.1212\ln(x) + 7.08$; $R^2 = 0{,}990$.

detection of pathologies.

CRediT authorship contribution statement

Quentin Palomar: Conceptualization, Investigation, Methodology, Visualization, Data curation, Formal analysis, Writing - original draft. **XingXing Xu:** Resources. **Robert Selegård:** Conceptualization, Resources, Writing - review & editing. **Daniel Aili:** Conceptualization, Supervision, Writing - review & editing, Funding acquisition. **Zhen Zhang:** Conceptualization, Supervision, Writing - review & editing, Funding acquisition.

Declaration of Competing Interest

The authors declare that they have no known competing financial interests or personal relationships that could have appeared to influence the work reported in this paper.

Acknowledgements

This work was supported by the Swedish Strategic Research Foundation (SSF FFL15-0174 and FFL15-0026), the Swedish Research Council (VR 2019-04690 and VR 2017-04475), and the Swedish Cancer Foundation (CAN 2017/430), the Swedish Government Strategic Research Area in Materials Science on Functional Materials at Linköping University (Faculty Grant SFO-Mat-LiU No. 2009-00971) and the Wallenberg Academy Fellow Program (KAW 2015.0127 and KAW 2016.0231). The authors want to thank Asta Makaraviciute for her collaboration.

Appendix A. Supplementary data

Supplementary material related to this article can be found, in the online version, at doi:https://doi.org/10.1016/j.snb.2020.128789.

References

[1] D. Grieshaber, et al., Electrochemical biosensors - sensor principles and architectures, Sensors 8 (2008) 1400–1458.
[2] X. Fan, et al., Sensitive optical biosensors for unlabeled targets: a review, Anal. Chim. Acta 620 (2008) 8–26.
[3] W.G. Stetler-Stevenson, R. Hewitt, M. Corcoran, Matrix metalloproteinases and tumor invasion: from correlation and causality to the clinic, Semin. Cancer Biol. 7 (1996) 147–154.
[4] J.R. MacDougall, L.M. Matrisian, Contributions of tumor and stromal matrix metalloproteinases to tumor progression, invasion and metastasis, Cancer Metastasis Rev. 14 (1995) 351–362.
[5] R. Lichtinghagen, et al., Matrix metalloproteinase (MMP)-2, MMP-7, and tissue inhibitor of metalloproteinase-1 are closely related to the fibroproliferative process in the liver during chronic hepatitis C, J. Hepatol. 34 (2001) 239–247.
[6] S.P. Hawkes, H. Li, G.T. Taniguchi, Zymography and reverse zymography for detecting MMPs and TIMPs, Methods Mol. Biol. 622 (2010) 257–269.
[7] F.S.H. Krismastuti, S. Pace, N.H. Voelcker, Porous silicon resonant microcavity biosensor for matrix metalloproteinase detection, Adv. Funct. Mater. 24 (2014) 3639–3650.
[8] K.R. Rogers, Principles of affinity-based biosensors, Affinity-Based Biosensors 109, Mol. Biotechnol. 14 (2000).
[9] J. Wang, Electrochemical biosensors: towards point-of-care cancer diagnostics, Biosens. Bioelectron. 21 (2006) 1887–1892.
[10] A. Biela, et al., Disposable MMP-9 sensor based on the degradation of peptide cross-linked hydrogel films using electrochemical impedance spectroscopy, Biosens. Bioelectron. 68 (2015) 660–667.
[11] D. Wang, Y. Yuan, Y. Zheng, Y. Chai, R. Yuan, An electrochemical peptide cleavage-based biosensor for matrix metalloproteinase-2 detection with exonuclease III-assisted cycling signal amplification, Chem. Commun. (Camb.) 52 (2016) 5943–5945.
[12] G. Liu, J. Wang, D.S. Wunschel, Y. Lin, Electrochemical proteolytic beacon for detection of matrix metalloproteinase activities, J. Am. Chem. Soc. 128 (2006) 12382–12383.
[13] Y. Zheng, Z. Ma, Dual-reaction triggered sensitivity amplification for ultrasensitive peptide-cleavage based electrochemical detection of matrix metalloproteinase-7, Biosens. Bioelectron. 108 (2018) 46–52.
[14] M. Holzinger, A. Goff, S. Le & Cosnier, Nanomaterials for biosensing applications: a review, Front. Chem. 2 (2014) 63.
[15] P. Chen, R. Selegård, D. Aili, B. Liedberg, Peptide functionalized gold nanoparticles for colorimetric detection of matrilysin (MMP-7) activity, Nanoscale 5 (2013) 8973.
[16] J. Wang, Carbon-nanotube based electrochemical biosensors: a review, Electroanalysis 17 (2005) 7–14.
[17] D. Zhu, et al., A free-standing and flexible phosphorus/nitrogen dual-doped three-dimensional reticular porous carbon frameworks encapsulated cobalt phosphide with superior performance for nitrite detection in drinking water and sausage samples, Sensors Actuators, B Chem. 321 (2020), 128541.
[18] J.A. Cruz-Navarro, F. Hernandez-Garcia, G.A. Alvarez Romero, Novel applications of metal-organic frameworks (MOFs) as redox-active materials for elaboration of carbon-based electrodes with electroanalytical uses, Coord. Chem. Rev. 412 (2020).
[19] a Bogomolova, et al., Challenges of electrochemical impedance spectroscopy in protein biosensing challenges of electrochemical impedance spectroscopy in protein biosensing, Anal. Chem. 81 (2009) 3944–3949.
[20] Palomar, Q. et al. Voltammetric sensing of recombinant viral dengue virus 2 NS1 based on Au nanoparticle-decorated multiwalled carbon nanotube composites. doi: 10.1007/s00604-020-04339-y.
[21] A. Carpenter, I. Paulsen, T. Williams, Blueprints for biosensors: design, limitations, and applications, Genes (Basel). 9 (2018) 375.
[22] K. Scott, Electrochemical principles and characterization of bioelectrochemical systems. Microbial Electrochemical and Fuel Cells, Elsevier, 2016, pp. 29–66.
[23] M. Dijksma, B.A. Boukamp, B. Kamp, W.P. Van Bennekom, Effect of hexacyanoferrate(II/III) on self-assembled monolayers of thioctic acid and 11-mercaptoundecanoic acid on gold, Langmuir 18 (2002) 3105–3112.
[24] S. Vogt, Q. Su, C. Gutiérrez-Sánchez, G. Nöll, Critical view on electrochemical impedance spectroscopy using the Ferri/Ferrocyanide redox couple at gold electrodes, Anal. Chem. 88 (2016) 4383–4390.
[25] M. Yaguchi, T. Uchida, K. Motobayashi, M. Osawa, Speciation of adsorbed phosphate at gold electrodes: a combined surface-enhanced infrared absorption spectroscopy and DFT study, J. Phys. Chem. Lett. 7 (2016) 3097–3102.
[26] K.Y. Foo, B.H. Hameed, Insights into the modeling of adsorption isotherm systems, Chem. Eng. J. 156 (2010) 2–10.

[27] D. Wang, Y. Chai, Y. Yuan, R. Yuan, A peptide cleavage-based ultrasensitive electrochemical biosensor with an ingenious two-stage DNA template for highly efficient DNA exponential amplification, Anal. Chem. 89 (2017) 8951–8956.
[28] B.B. Kou, et al., DNA enzyme-decorated DNA nanoladders as enhancer for peptide cleavage-based electrochemical biosensor, ACS Appl. Mater. Interfaces 8 (2016) 22869–22874.
[29] H. Gao, et al., Highly selective electrogenerated chemiluminescence biosensor for simultaneous detection of matrix metalloproteinase-2 and matrix metalloproteinase-7 in cell secretions, Sensors Actuators B Chem. 253 (2017) 69–76.
[30] Z. Wei, H. Wang, Z. Ma, H. Han, Amperometric biosensor of matrix metalloproteinase-7 enhanced by Pd-functionalized carbon nanocomposites, Nanoscale Res. Lett. 13 (2018).
[31] Z. Lei, H. Zhang, Y. Wang, X. Meng, Z. Wang, Peptide microarray-based metal enhanced fluorescence assay for multiple profiling of matrix metalloproteinases activities, Anal. Chem. 89 (2017) 6749–6757.
[32] W. Zhuang, Y. Li, J. Chen, W. Liu, H. Huang, Copper nanocluster-labeled hybridization chain reaction for potentiometric immunoassay of matrix metalloproteinase-7 in acute kidney injury and renal cancer, Anal. Methods 11 (2019) 2597–2604.
[33] C. Ress, et al., Influence of significant weight loss on serum matrix metalloproteinase (MMP)-7 levels, Eur. Cytokine Netw. 21 (2010) 65–70.
[34] G. Sarkissian, et al., Identification of pro-MMP-7 as a serum marker for renal cell carcinoma by use of proteomic analysis, Clin. Chem. 54 (2008) 574–581.
[35] T. Szarvas, et al., Urinary matrix metalloproteinase-7 level is associated with the presence of metastasis in bladder cancer, BJU Int. 107 (2011) 1069–1073.
[36] M. El Demery, et al., Serum matrix metalloproteinase-7 is an independent prognostic biomarker in advanced bladder cancer, Clin. Transl. Med. 3 (2014).

Quentin Palomar has joined the group “Biosystèmes Electrochimiques & Analytiques” (BEA) headed by Dr. Serge Cosnier at the DCM unit of the University of Grenoble as a PhD student in 2014. In 2017, he completed his Ph.D. in biosensor design entitled: Integration of nanostructured materials in the design and realization of label-free biosensors for detection of targets of interest. In 2018, he joined Professor Zhen Zhang’s group as a postdoctoral researcher. His current work focuses on the design of biosensors based on silicon nanowire and on electrochemical detection of biomolecules.

XingXing Xu started as a PhD student in Uppsala University in 2015 and is now part of Professor Zhen Zhang group as a postdoctoral researcher. Her research focuses on the study of electrochemical phenomena, the design and realization of electrochemical biosensors and the study of surface as well as the fabrication of nanostructures.

Robert Selegård is an assistant professor at the University of Linköping and more particularly in the Department of Physics, Chemistry and Biology (IFM). His research is primarily focused on the use and development of peptides for various applications, including biosensors.

Daniel Aili research interests involve design and development of molecules, soft materials and hybrid nanoscale components and devices for a wide range of applications in biomedicine and molecular biology; including diagnostics, biosensors, drug delivery and regenerative medicine. He has also large interest in molecular self-assembly an in fundamental self-assembly processes, in oder to develop bioresponsive and biointeractive materials and devices with different compositions, nanostructures, and functions.

Prof. Zhen Zhang is currently a professor in electronics at the Angstrom laboratory, Uppsala University, Sweden and an adjunct researcher with IBM T. J. Watson Research Center, Yorktown Heights, NY. Before joining Uppsala University as a tenure track assistant professor in Aug. 2013, he was a postdoctoral research fellow (2008–2010) then a Research Staff Member (2010−2013) at IBM T. J. Watson Research Center. Dr. Zhang received his Ph.D degree from the Royal Institute of Technology (KTH), Sweden in 2008. He got the M.Sc degree at Shanghai Institute of Ceramics, Chinese Academy of Sciences in 2003 and the B.Sc. degree at University of Science and Technology of China (USTC) in 2000.